ISSN 2029-6991 / eISSN 2029-7009

VILNIUS TECH
Vilnius Gediminas Technical University

GEODESY and CARTOGRAPHY

2026
Volume 52
Issue 1
Pages 1–10
https://doi.org/10.3846/gac.2026.22447

UDC 528.8.04

PREDICTION OF TERRESTRIAL WATER STORAGE CHANGES BY USING GRACE DATA OVER NILE RIVER BASIN

Basma FAWZI[1]✉, Mahmoud SALAH[2], Mahmoud EL-MEWAFI[3]

[1]*Department of Civil Engineering, Delta Higher Institute for Engineering and Technology, 35111 Mansoura, Egypt*
[2]*Department of Geomatics, Faculty of Engineering Shoubra, Benha University, 13518 Banha, Egypt*
[3]*Public Works Department, Faculty of Engineering, Mansoura University, 35111 Mansoura, Egypt*

Article History:
- received 14 October 2024
- accepted 29 November 2025

Abstract. This research involved training two deep learning prediction models: Long Short-Term Memory (LSTM) and Dipper Throated Optimizations Fitness Grey Wolf-LSTM (DTOFGW-LSTM), utilizing data obtained from remote sensing to reconstruct and predict the Terrestrial Water Storage Changes (TWSC) over Nile River Basin (NRB). We evaluated factors including Terrestrial Water Storage Changes (TWSC) and Groundwater Storage Changes (GWSC), identified through the Gravity Recovery and Climate Experiment (GRACE) and GRACE-Follow-On (GRACE-FO), alongside precipitation data collected by the Global Precipitation Climate Change Program (GPCP) to analyze the patterns of change within the research area. We utilized the LSTM and DTOFGW-LSTM algorithms to rebuild the TWSC and GWSC from 2018 to 2024. We utilized the precise model to forecast the GRACE gap from 2017 to 2018 and the TWSC from 2024 to 2030. The findings demonstrated the superiority of the suggested model (DTOFGW-LSTM) with a root mean square error (RMSE) of 0.51, a coefficient of determination (R^2) of 0.99, and a mean absolute percentage error (MAPE) of 0.21.

Keywords: GRACE, GRACE-FO, DTOFGW-LSTM, LSTM, TWSC, GWSC.

✉Corresponding author. E-mail: ***basma.fawzi283@gmail.com***

1. Introduction

Recent data gathering techniques and algorithmic solutions provided by platforms such as GRACE (Gravity Recovery and Climate Experiment) and GRACE-FO (Follow-On) satellite data have started to yield further insights into the dynamics of water resources in the NRB (Awange et al., 2014; Hasan & Tarhule, 2020). The GRACE mission comprises two low-Earth orbiting satellites situated in the same orbital plane at an altitude of 450 km and an inclination of 89.5 degrees. The distance between the two satellites is accurately estimated using a K-band ranging device, while the position of each satellite is established by GPS receivers onboard the spacecraft (Tapley et al., 2004).

The GRACE satellite offers novel gravity data that enables the monitoring of changes in Terrestrial Water Storage (TWSC). TWSC is categorized into five components: groundwater, soil moisture, surface water, snow/ice water, and biological water storage (Strassberg et al., 2009). The Earth's climate system is significantly influenced by the vast range of spatio-temporal scale changes in TWS. TWS, or Total Water Storage, is a crucial strategic asset for any country. It serves as the foundation for agricultural irrigation, industrial output, urban water supply, and the upkeep of the ecological environment. Hence, the precise forecasting of TWSC holds immense importance for water resource management, drought and disaster risk assessment, and the advancement of coordinated development of the ecological environment (Duan et al., 2024).

Multiple studies have been carried out to reconstruct the Total Water Storage (TWS) utilizing various datasets and methodologies, encompassing both grid and basin scales. The TWS_{GRACE} reconstruction has utilized hydroclimatic or gravimetric datasets, both measured and modeled (Gyawali et al., 2022). The hydroclimate variables were utilized to reconstruct TWS by establishing a correlation between the spatial and temporal variations in these variables and the spatial and temporal variations in TWS. Some examples of climatic variables are temperature, rainfall, sea surface temperature, and climate indices (Ahmed et al., 2019). Hydrological factors including soil moisture, runoff, water level, and evapotranspiration (Llovel et al., 2010; Long et al., 2014; Pan et al., 2012).

In order to anticipate the effects of future changes in the earth system on (TWSC) and (GWSC), it is important to measure the relationship between changes in climate,

surface water extent, hydrological components, and vegetation in order to understand how groundwater responds to these changes (Sahoo et al., 2017).

Recently, advanced deep learning models, including the Long Short-Term Memory (LSTM) model, a type of Recurrent Neural Network (RNN), and the Convolutional Neural Network (CNN) model, have been created to address complex and nonlinear prediction tasks with long-term dependencies. These models have demonstrated impressive performance (Wang et al., 2021).

This study utilized two deep learning models in conjunction with remote sensing data to accurately predict spatiotemporal changes in Terrestrial Water Storage (TWSC) and Groundwater Storage (GWSC). The remote sensing data provided continuous and geographical information, enhancing the accuracy of the predictions. This study aimed to construct LSTM and DTOFGW-LSTM deep learning models to predict GWSC and TWSC from multi-satellite data and photos, considering the potential effectiveness of combining deep learning models with remote sensing image data.

2. Materials and methods

2.1. Study area

The Nile River basin (NRB; approximately 3.18 million km^2) constitutes a complicated transboundary hydrological system (Shahin, 1985). The Nile is the longest river in the world, flowing for 6,850 kilometers. It is also the second largest river by watershed area, behind only the Amazon. The confluence of the White and Blue Nile rivers causes the Nile to flow northward from southward, making it unique among African rivers. The entire runoff at Aswan High Damin, Egypt, is projected to be over 88.5 billion cubic meters per year, according to the typical natural water flow in the Nile. There are four primary sub-basins that make up the Nile basin: the White Nile Basin (WNB), the BNB, the Atbara River Basin, and the main or trunk stem Nile Basin. The NRB is inhabited by around 320 million individuals from 11 African states, according to 2018 population estimates, constituting approximately 24% of Africa's overall population (Hasan et al., 2021). Figure 1 shows the location of NRB throughout Africa continent.

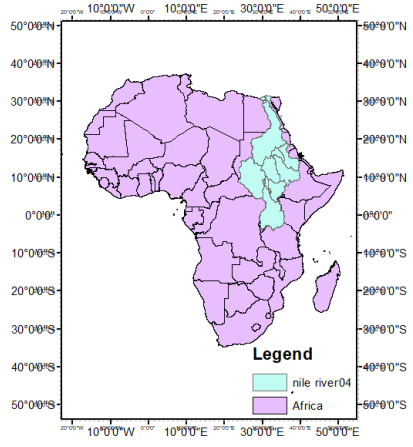

Figure 1. Location of the study area (was generated by ArcMap 10.8.2 sofware)

2.2. Data used

2.2.1. GRACE Mascon data

Earth's gravitational field models are commonly distributed in two types of products: spherical harmonic coefficient products and Mascon products (Loomis et al., 2021). Prior to their utilization in research, conventional spherical harmonic coefficient products necessitate additional processing steps, including the substitution and supplementing of low-order terms, the elimination of stripes, and the correction for Glacial Isostatic Adjustment (GIA). The Gravity field Mascon products address the limitations of the ball harmonic coefficient products by effectively addressing the north-south strip error noise, correcting leakage error, and providing GIA correction without the need for post-processing. Users can directly utilize these goods. Mascon is able to accurately determine changes in mass at increased levels of spatial and temporal resolution. This capability has resulted in a diverse variety of applications for Mascon in areas such as polar ice caps, alpine glaciers, hydrology, and seas. Zhang and Sun (2021) highlighted that the Mascon product is specifically designed to eliminate the need for post-processing and address the leakage errors that arise from filtering traditional spherical harmonic coefficients. It is particularly well-suited for accurately estimating mass changes in various layers of the Earth system.

Scanlon et al. (2018) conducted a comprehensive evaluation of the results of CSR's and JPL's Mascon products for estimating terrestrial water storage in 176 basins worldwide. They found that the Mascon products were more accurate in recovering hydrologic-gravity signals compared to traditional spherical harmonic coefficient products. Currently, there are three worldwide organizations, namely JPL, CSR, and GSFC, that are publishing mascon products.

This research utilizes the GRACE RL06 v02 mascon product, which was published by the Center for Space Research (CSR) at the University of Texas, USA. The CSR mascon product has a spatial resolution of 0.25. This research extracted a total of 163 months of TWSC time series from April 2002 to June 2017 as an input data, excluding any missing months as indicated by the CSR RL06 Mascon product, this data as shown in Figure 2 represents samples of TWSC over NRB which have been extracted from Netcdf format of the time series data of the GRACE mission and Figure 3 shows the value of TWSC over NRB during the period from 2002 to 2017 which have been generated using ArcMap 10.5 program. The GRACE & GRACE-FO data is available at the web site as shown in Table 1. The GRACE data is not available during the period from July 2017 to June 2018 (Gap period) as shown in Figure 4. The GRACE time series data for GWSC over NRB as shown in Figure 5 during the study period (2002–2017).

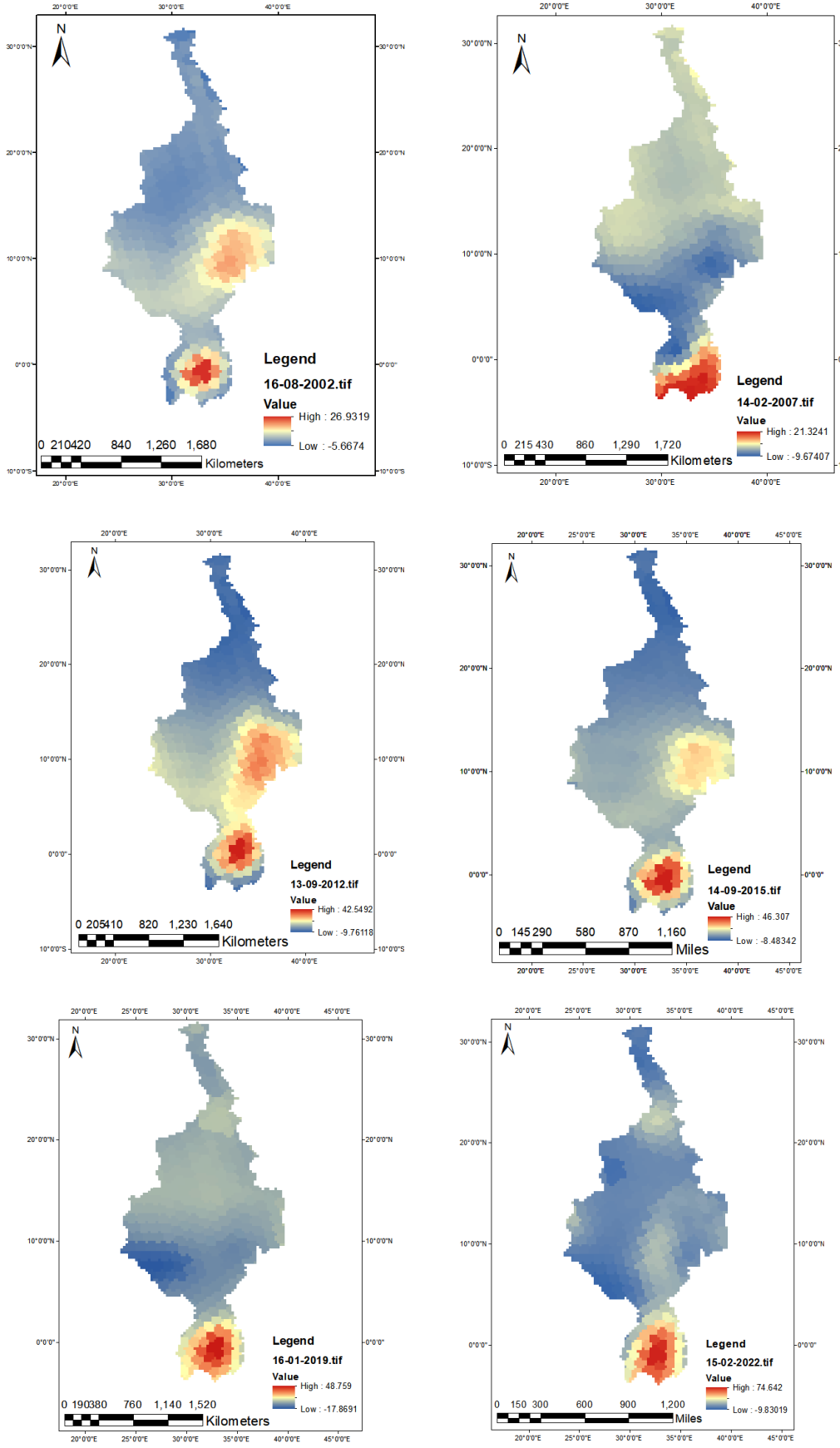

Figure 2. Samples of time series Geotiff data

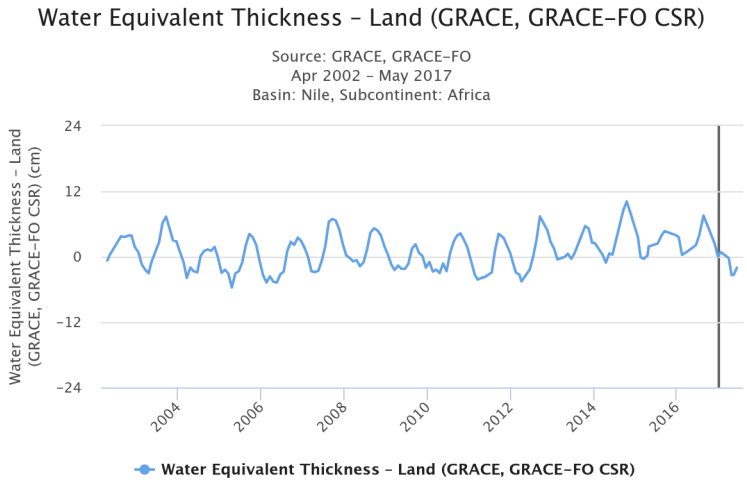

Figure 3. TWSC during the period (2002–2017)

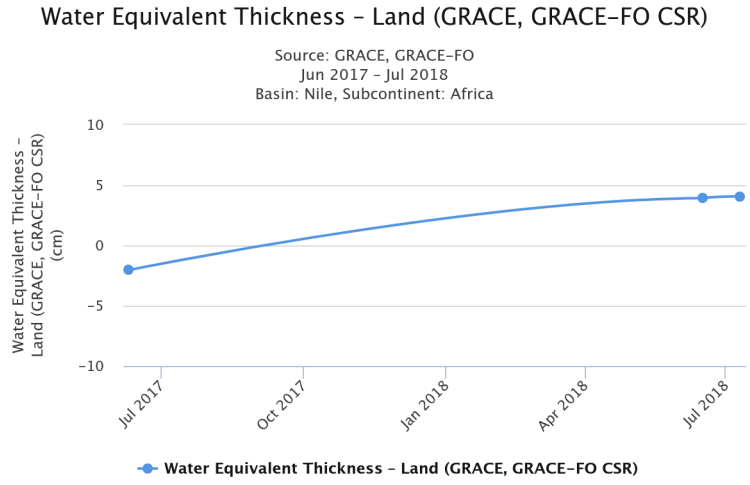

Figure 4. Gap period of GRACE data (2017–2018)

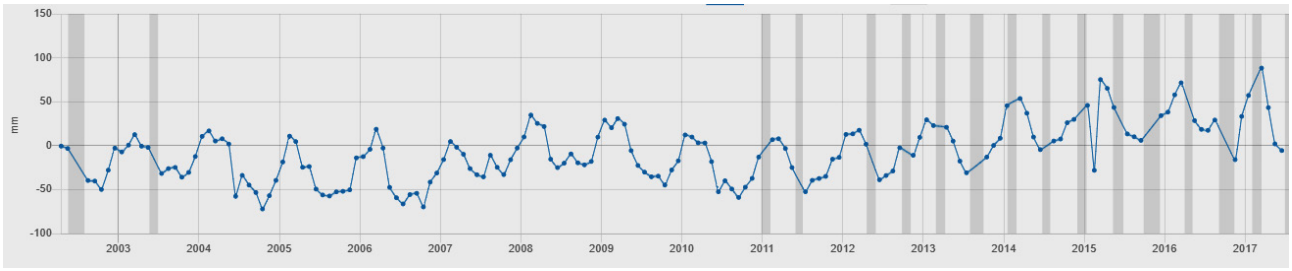

Figure 5. GWSC during the period (2002–2017)

2.2.2. Precipitation and temperature data

We employed long-term precipitation data from 1901 to 2020 sourced from the GPCC (Global Precipitation Climatology Centre) gridded gauge-analysis precipitation products. The statistics were sourced from the Deutscher Wetterdienst (DWD), the German Meteorological Service. The GPCC offers global monthly gauge-corrected precipitation products at a 0.5 × 0.5 grid size. The long-term monthly records of precipitation, temperature, and potential evapotranspiration (PET) were sourced from time-series datasets provided by the Climate Research Unit (CRU) at the University of East Anglia, UK. The CRU data were computed at a resolution of 0.5 by 0.5, utilizing over 4000 meteorological stations globally (Belda et al., 2015). The data of precipitation and temperature are available as shown in Table 1. The average precipitation over the study area (NRB) of the input data during the period (2002–2017) as shown in Figure 6.

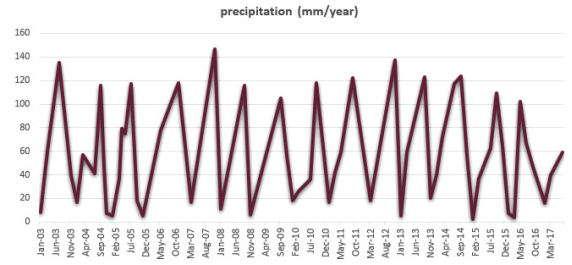

Figure 6. Average precipitation over NRB

Table 1. Websites of the data used

Data Types	Data	Websites
GRACE & GRACE-FO (TWSC)	CSR (RL06)	http://www2.csr.utexas.edu/grace
GRACE & GRACE-FO (G3P)	GFZ (RL06)	http://gravis.gfz-potsdam.de/gws
Precipitation	GPCP	http://gpcc.dwd.de/
Temperature	CRU	https://climatedataguide.ucar.edu/climate-data/global-temperature-data-sets-overview-comparison-table

2.3. Models used

This Section describes the models used in the reconstructing and predicting the TWSC over the study area during the period 2018 to 2030 using two deep learning LSTM and DTOFGW-LSTM models.

2.3.1. LSTM

LSTM is a prevalent deep learning technique utilized for regression, particularly in time-series forecasting, and it addresses the vanishing gradient issue in long-term predictions. LSTM is marginally more intricate than the conventional RNN in computing hidden states and incorporates cell memory. In the LSTM cell memory, three types of gates (input gates, forget gates, and output gates) eliminate superfluous memories and ascertain what the network shouldretain. LSTM possesses a conveyor-belt-like architecture comprising cell states, with each cell state featuring a learner for state updates (Zhang et al., 2018). The building of LSTM model according to Lu et al. (2024) as shown in Figure 7.

2.3.2. DTOFGW-LSTM

The proposed model is a synthesis of two methodologies: Dipper Throated Optimizations (DTO) and Fitness of Grey Wolf Optimizations (GWO), aimed at selecting the most effective parameters for this study. The parameters of the proposed model (DTOFGW) are detailed in Table 2. According to Pan et al. (2020) the optimization strategy, the number of training iterations, and other model variables and hyperparameter settings are enhanced through the DTO algorithm. The cross-validation process employs a dictionary containing predefined parameters with specified value ranges to perform a randomized search, with the objective of identifying the most suitable parameters for LSTM.

2.4. Performance measures

2.4.1. Root means square error

The Root-Mean-Square-Error (RMSE) is calculated by taking the square root of the ratio of the square of the difference between the predicted and true values, divided by the total number of observations, which is k. An observation's divergence from its real value can be measured using the root mean square error. The lower the Root-Mean-Squared Error (RMSE) value, the more accurate the results are since there is less of a discrepancy between the sequence of simulated values and the sequence of ob-

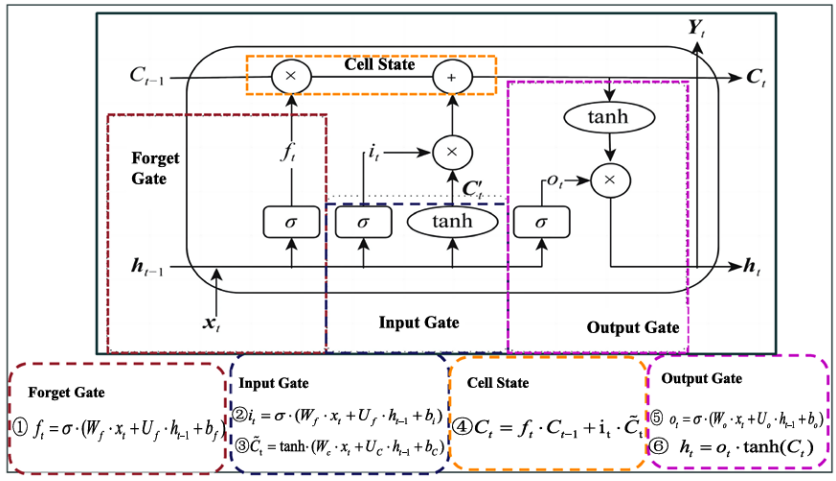

Note: $x = [x_1, x_2, ..., x_n]$ represents the input data. The input gate i_t serves as the mechanism for retaining current knowledge, g_t retains the revised information, σ is the activation function, *W* is the weight, *h* is the hidden state, b is the bias term, The forget gate f_t deletes memories, the x_t and the hidden state at $t - 1$ (h_{t-1}) pass through the activation function. The input gate and forget gate determine the new memory cell state (C_t) by an elementwise product.

Figure 7. The architecture of the LSTM model unit according to Lu et al. (2024)

Table 2. The proposed method of DTOFGW

The suggested DTOFGW method
Get started Birds' Distribution $(BD)_i$ $(i = 1, 2, 3, 4, \ldots\ldots, s)$ with size n, BS_i $(i = 1, 2, 3, \ldots, s)$, Fitness assessment Fs, f_s, r_1, r_2, r_3, R, C_1, C_2, C_3, C_4, C_5, t=1, and max iterations $\_max_{iter}$
Evaluate Fitness assessment Fs for each $(BD)_i$
Find best bird BD_{BEST}
While t < iter_max **do**
for (i =1; i ≤ s) **do**
If (Z < 0.5) **then**
Update The gey wolf operatives' position as determined by:
Update (fitness)Strength training $\overrightarrow{F\alpha} = (\vec{F}_\alpha / (\vec{F}_\alpha + \vec{F}_\beta + \vec{F}_\delta)$
Update (fitness)Strength training $\vec{F}_\beta = (\vec{F}_\alpha / (\vec{F}_\alpha + \vec{F}_\beta + \vec{F}_\delta)$
Update (fitness)Strength training $\vec{F}_\delta = (\vec{F}_\alpha / (\vec{F}_\alpha + \vec{F}_\beta + \vec{F}_\delta)$
$\vec{W}_\alpha = \lvert\vec{W}_1 \times \vec{F}_\alpha - \vec{F}\rvert$, $\overrightarrow{WD}_\beta = \lvert\vec{W}_2 \times \vec{F}_\beta - \vec{F}\rvert$, $\overrightarrow{WD}_\delta = \lvert\vec{W}_3 \times \vec{F}_\delta - \vec{F}\rvert$
else
Update The flying Velocity of bird applying:
$BS(m+1) = C_3 BS(m) + C_4 r_1 (BD_{BEST}(m) - BD_{st.nd}(m)) + C_5 r_1 (BD_{G.BEST} - BD_{st.nd}(m))$
Update The swimming bird's position as determined by: $BD_{st.nd}(m+1) = r_1 + z \times r_2 + (1-z) \times r_3 + BS(m+1)$
end after
end after
Evaluate Fitness assessment Fs for each $\overrightarrow{BD_i}$
Update R, r_1, r_2, r_3, c, C_1, C_2
Find best bird BL_{best}
Set $BD_{G.BEST}$ = BD_{BEST}
Set m = m + 1
end when
return $BL_{G.BEST}$

served values. Here is the equation:

$$RMSE = \sqrt[2]{\frac{1}{K}\sum_{i=1}^{K}(X_i - \grave{X}_i)}, \quad (1)$$

where K represents the number of samples, X_i signifies the true value of the i-th sample, and $\grave{X}_i$ indicates the predicted value of the i-sample.

2.4.2. Coefficient of determination

The coefficient of determination (R^2) is a statistic that quantifies the degree of fit. As R^2 approaches 1, it indicates that the regression line provides a good fit to the observations; on the other hand, a smaller value indicates a poor fit. Let me give you the equation:

$$R^2 = 1 - \frac{\sum_{i=1}^{K}(X_i - \grave{X}_i)}{\sum_{i=1}^{K}(X_i - \overline{X}_i)}, \quad (2)$$

where K represents the number of samples, X_i signifies the actual observed value of the i-th sample, $\grave{X}_i$ indicates the predicted value of the i-th sample, and $\overline{X}_i$ symbolizes the mean of the actual observed values.

2.4.3. Mean absolute percentage error

The Mean Absolute Percentage Error (MAPE) is frequently employed to quantify prediction accuracy, particularly in the context of time series forecasting. The equation for calculation is as follows:

$$MAPE = \frac{100\%}{k}\sum_{i=1}^{K}\left|\frac{\grave{X}_i - X_i}{X_i}\right|, \quad (3)$$

where K represents the number of samples, X_i signifies the true value of the i-th sample, and $\grave{X}_i$ symbolizes the predicted value of the i-th sample.

3. Results and discussion

This Section highlights the results of experiments aimed at assessing the efficacy of the proposed model (DTOFGW-LSTM) and LSTM in recreating groundwater storage variations and terrestrial water storage fluctuations from 2017 to 2024. Utilizing the superior model of the two to forecast data for the Gap period (2017–2018) and the subsequent years (2024–2030).

3.1. Reconstruction of TWSC

In this research, two artificial intelligence models (LSTM and DTOFGW-LSTM) were used to reconstruct TWSC data over NRB. Data taken from the GRACE and GRACE-FO between 2002 and 2018 were used as inputs data to runout the two models. The TWSC data was reconstructed in the period from 2018 to 2024 using LSTM model as shown in Figure 8 and using the proposed modified model (DTOFGW-LSTM), and the results were as shown in Figure 9. When analyzing the data from the two models, the results proved the superiority of the proposed model as follows: The proposed model (DTOFGW-LSTM) demonstrated superiority over previous models, with a Root Mean Square Error (RMSE) of 0.0.51, a Mean Absolute Percentage Error (MAPE) of 0.06, and a coefficient of determination (R^2) of 0.9937, as illustrated in Figure 10a. This model is a linear polynomial (y = 1.022x – 0.0673), where y refers to estimated TWSC obtained from the proposed model (DTOFGW-LSTM) and x is the measured TWSC from GRACE data. Figure 10b shows the relation between the TWSC from LSTM model (Estimated) and TWSC from GRACE time series data, the RMSE for this model equal 0.6, the value of MAPE equal 0.34 and R^2 equal 0.9796. LSTM algorithm is a linear polynomial (y = 1.0368x – 0.0569), where y is the estimated TWSC using LSTM model and x the measured data of TWSC over NRB during the period 2018–2024.

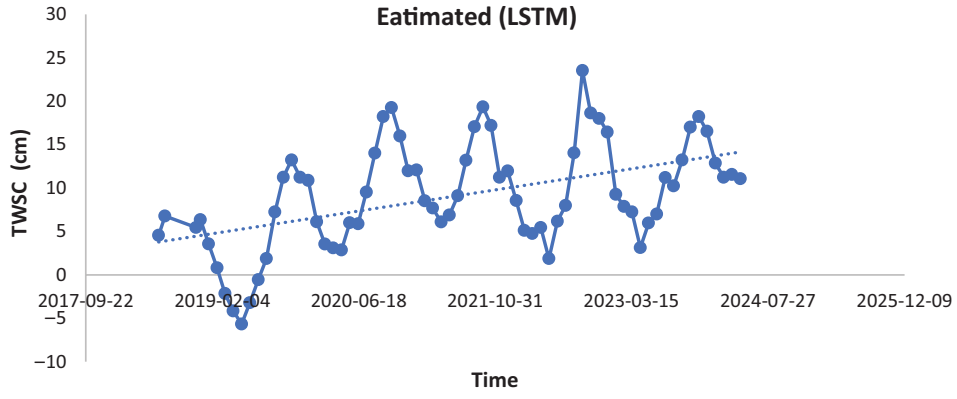

Figure 8. TWSC from (LSTM) model during the period (2018–2024)

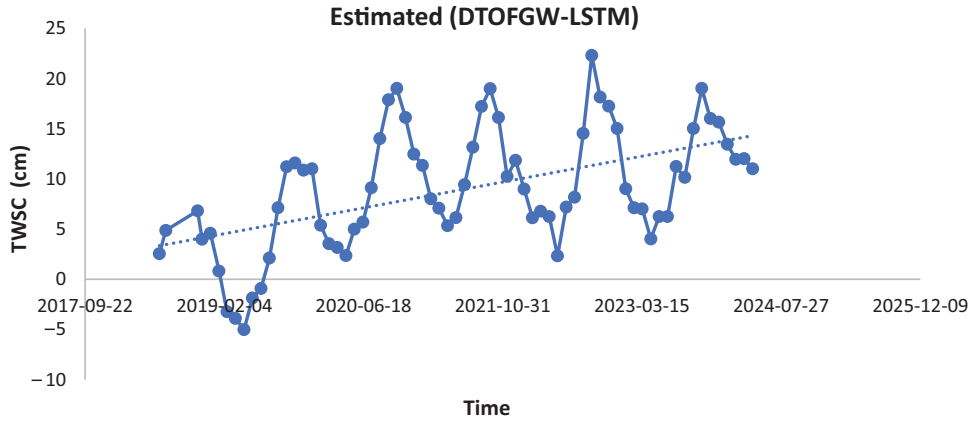

Figure 9. TWSC from (DTOFGW-LSTM) model during the period (2018–2024)

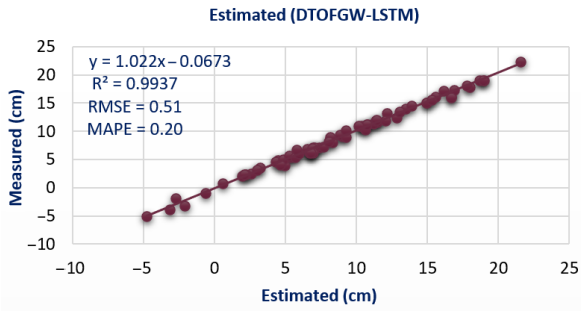

a)

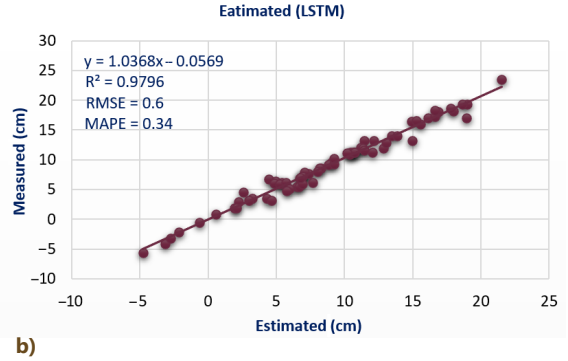

b)

Figure 10. TWSC (LSTM) during the period (2018–2024): a) Scatter chart for (DTOFGW-LSTM); b) Scatter chart for (LSTM)

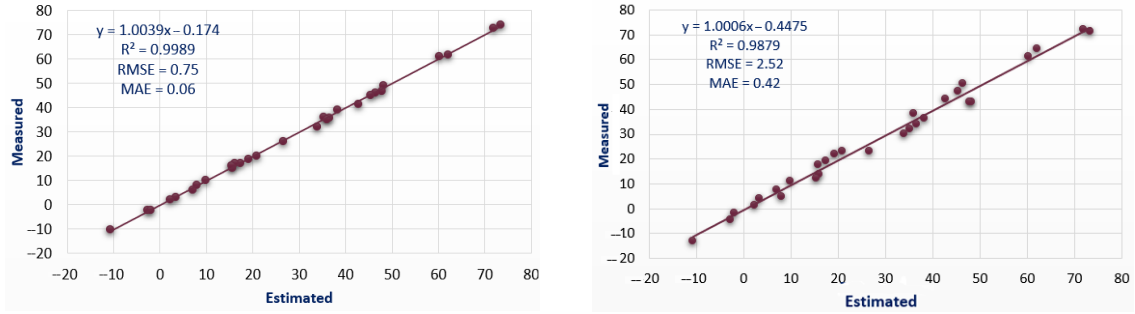

a) b)

Figure 11. Scatter chart for two models: a) LSTM algorithm; b) DTOFGW-LSTM

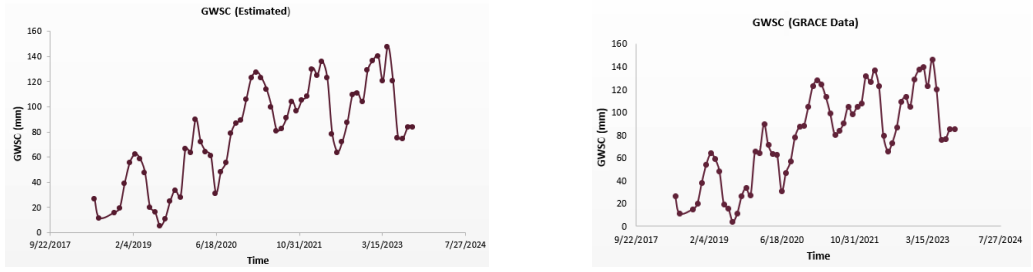

a) b)

Figure 12. GWSC during the period (2018–2024): a) GWSC from the proposed model (DTOFGW-LSTM); b) GWSC from (LSTM)

3.2. Reconstruction of GWSC

The proposed model (DTOFGW-LSTM) and LSTM model were applied for reconstructing the GWSC during the period 2018 to 2024. Figure 11a shows that the proposed model, DTOFGW-LSTM, outperormed the others with an RMSE of 0.75, an MAE of 0.06, and an R^2 of 0.9989. The estimated GWSC (y) is the result of the suggested model (DTOFGW-LSTM), and the observed GWSC (x) is the coefficient of this linear polynomial model. Figure 11b displays the correlation between the GWSC observed data and the LSTM model data. The results demonstrate that the model has an RMSE of 2.52, an R^2 value of 0.9879, and an MAE value of 0.42, where y is the estimated GWSC using the LSTM model and x is the observed data, the LSTM algorithm is a linear polynomial (y = 1.0006x – 0.4475). The reconstructing data of GWSC over the study area during the period (2018–2024) using the LSTM model as shown in Figure 12a and the GWSC during the same period using the proposed model as shown in Figure 12b.

3.3. The GRACE data gap forecasting

The suggested model (DTOFGW-LSTM) was employed to ascertain TWSC data throughout the GRACE GAP period from 2017 to 2018 (about one year), with TWS variations ranging from 0.17927 mm to 14.03725 mm, as illustrated in Figure 13.

3.4. Data forecasting for the coming years

After using the proposed model (DTOFGW-LSTM) in reconstructing TWSC and GWSC over the NRB during the period from 2018 to 2024, this model is prepared for doing the prediction in future over NRB during the period from 2024 to 2030. The proposed model was used because it showed a very high accuracy rate in the process of reconstructing TWSC data and the extent of matching the results obtained from it with the actual GRACE data in the period between 2018 to 2024. The results related to the prediction of future groundwater

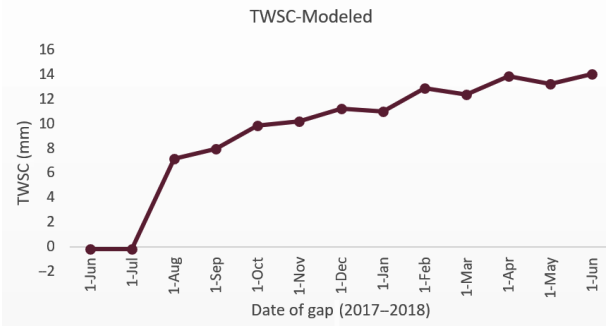

Figure 13. Data of TWSC during gap period (2017–2018)

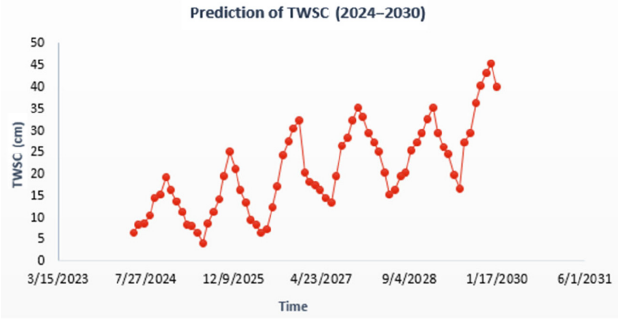

Figure 14. TWSC during the period (2018–2024)

storage in the period from May 2024 to January 2030 (approximately 69 months) were obtained from the proposed model as shown in Figure 14. The projected period of six years indicates a progressive increase in groundwater supply, exhibiting variable rates of growth. Notably, the water stock rises throughout the months of July, August, September, and October, peaking in November and December. From February to June, there is a decline in the groundwater level.

4. Conclusions

The principal aim of this research was to reconstruct GRACE and GRACE-FO data for the Nile River Basin (NRB) utilizing an extensive time series dataset spanning from 2002 to 2024, while examining the incidence of drought within the study area during the GAP period. This analysis was predicated on lunar data from the years preceding and succeeding the GAP period, alongside meteorological data concerning temperature and precipitation in the study area during the GAP period. This research depends on two artificial intelligence models (LSTM and DTOFGW-LSTM), these models first were used to reconstruct the GRACE data of TWSC and GWSC during the period (2018 to 2024) depending on the data of TWSC and GWSC from GRACE mission and the meteorological data of temperature and precipitation during the period from 2002 to 2017 as the input data to runout the models of artificial intelligence reconstructing data for TWSC and GWSC were obtained during the period from 2018 to 2024 the value of RMSE of the proposed model (DTOFGW-LSTM) for reconstructing TWSC and GWSC equal 0.51 and 0.75 respectively with value of coefficient of determination R^2 equal 0.9937 and 0.9979 respectively and The Mean Absolute Percentage Error MAPE equal 0.2 for reconstructing TWSC data during 2018 to 2024. The proposed model showed high accuracy of the data obtained so it was used to predict GRACE data during the Gap period (2017–2018). After that, the proposed model (DTOFGW-LSTM) was applied for predicting TWSC over NRB during the period from 2024 to 2030. The results obtained showed an increase in TWSC during this period. It was also noted that the months of July, August, September and October represent an increase in the level of TWSC and the peak for each year is in the months of November and December. It was also noted that there is a decrease during the months of March, April, May and June.

References

Ahmed, M., Sultan, M., Elbayoumi, T., & Tissot, P. (2019). Forecasting GRACE data over the African watersheds using artificial neural networks. *Remote Sensing*, *11*(15), Article 1769. https://doi.org/10.3390/rs11151769

Awange, J. L., Forootan, E., Kuhn, M., Kusche, J., & Heck, B. (2014). Water storage changes and climate variability within the Nile Basin between 2002 and 2011. *Advances in Water Resources*, *73*, 1–15. https://doi.org/10.1016/j.advwatres.2014.06.010

Belda, M., Halenka, T., Holtanová, E., Kalvová, J., & Hlávka, Z. (2015). Evaluation of CMIP5 present climate simulations using the Köppen-Trewartha climate classification. *Climate Research*, *64*, 201–212. https://doi.org/10.3354/cr01316

Duan, A., Zhong, Y., Xu, G., Yang, K., Tian, B., Wu, Y., Bai, H., & Hu, E. (2024). Quantifying the 2022 extreme drought in the Yangtze River Basin using GRACE-FO. *Journal of Hydrology*, *630*, Article 130680. https://doi.org/10.1016/j.jhydrol.2024.130680

Gyawali, B., Ahmed, M., Murgulet, D., & Wiese, D. N. (2022). Filling temporal gaps within and between GRACE and GRACE-FO terrestrial water storage records: An innovative approach. *Remote Sensing*, *14*(7), Article 1565. https://doi.org/10.3390/rs14071565

Hasan, E., & Tarhule, A. (2020). GRACE: Gravity recovery and climate experiment long-term trend investigation over the Nile River Basin: Spatial variability drivers. *Journal of Hydrology*, *586*, Article 124870. https://doi.org/10.1016/j.jhydrol.2020.124870

Hasan, E., Tarhule, A., & Kirstetter, P. (2021). *Using GRACE/GRACE-FO, data-driven and modeling to access the twentieth and twenty-first century water storage changes in the Nile River Basin*. Preprints. https://doi.org/10.20944/preprints202101.0357.v1

Llovel, W., Becker, M., Cazenave, A., Crétaux, J.-F., & Ramillien, G. (2010). Global land water storage change from GRACE over 2002–2009; Inference on sea level. *Comptes Rendus Géoscience*, *342*(3), 179–188. https://doi.org/10.1016/j.crte.2009.12.004

Long, D., Shen, Y., Sun, A., Hong, Y., Longuevergne, L., Yang, Y., Li, B., & Chen, L. (2014). Drought and flood monitoring for a large karst plateau in Southwest China using extended GRACE data. *Remote Sensing of Environment*, *155*, 145–160. https://doi.org/10.1016/j.rse.2014.08.006

Loomis, B. D., Felikson, D., Sabaka, T. J., & Medley, B. (2021). High-spatial-resolution mass rates from GRACE and GRACE-FO: Global and ice sheet analyses. *Journal of Geophysical Research*: *Solid Earth*, *126*(12), Article e2021JB023024. https://doi.org/10.1029/2021JB023024

Lu, S., Li, W., Yao, G., Zhong, Y., Bao, L., Wang, Z., Bi, J., Zhu, C., & Guo, Q. (2024). The changes prediction on terrestrial water storage in typical regions of China based on neural networks and satellite gravity data. *Scientific Reports*, *14*, Article 16855. https://doi.org/10.1038/s41598-024-67611-8

Pan, M., Sahoo, A. K., Troy, T. J., Vinukollu, R. K., Sheffield, J., & Wood, E. F. (2012). Multisource estimation of long-term terrestrial water budget for major global river basins. *Journal of Climate*, *25*, 3191–3206. https://doi.org/10.1175/JCLI-D-11-00300.1

Pan, J., Jing, B., Jiao, X., & Wang, S. (2020). Analysis and application of grey wolf optimizer-long short-term memory. *IEEE Access*, *8*, 121460–121468. https://doi.org/10.1109/access.2020.3006499

Sahoo, S., Russo, T. A., Elliott, J., & Foster, I., (2017). Machine learning algorithms for modeling groundwater level changes in agricultural regions of the US. *Water Resources Research*, *53*(5), 3878–3895. https://doi.org/10.1002/2016WR019933

Scanlon, B. R., Zhang, Z., Save, H., Sun, A. Y., Schmied, H. M., Van Beek, L. P. H., Wiese, D. N., Wada, Y., Reedy, R. C., Longuevergne, L., Döll, P., & Bierkens, M. F. P. (2018). Global models underestimate large decadal decline and rising water storage trends relative to GRACE satellite data. *Proceedings of National Academy of Sciences of The United States of America*, *115*(6), E1080–E1089. https://doi.org/10.1073/pnas.1704665115

Shahin, M. M. A. (1985). *Hydrology of the Nile Basin* (Vol. 21). Elsevier.

Strassberg, G., Scanlon, B. R., & Chambers, D. (2009). Evaluation of groundwater storage monitoring with the GRACE satellite: Case study of the High Plains aquifer, central United States.

Water Resources Research, *45*(5), Article W05410. https://doi.org/10.1029/2008WR006892

Tapley, B. D., Bettadpur, S., Watkins, M., & Reigber, C. (2004). The gravity recovery and climate experiment: Mission overview and early results. *Geophysical Reserch Letters*, *31*(9), Article L09607. https://doi.org/10.1029/2004GL019920

Wang, F., Chen, Y., Li, Z., Fang, G., Li, Y., Wang, X., Zhang, X., & Kayumba, P. M. (2021). Developing a long short-term memory (LSTM)-based model for reconstructing terrestrial water storage variations from 1982 to 2016 in the Tarim river basin, Northwest China. *Remote Sensing*, *13*(5), Article 889. https://doi.org/10.3390/rs13050889

Zhang, J., Zhu, Y., Zhang, X., Ye, M., & Yang, J. (2018). Developing a Long Short-Term Memory (LSTM) based model for predicting water table depth in agricultural areas. *Journal of Hydrology*, *561*, 918–929. https://doi.org/10.1016/j.jhydrol.2018.04.065

Zhang, L., & Sun, W. (2022). Progress and prospects of GRACE Mascon product and its application. *Reviews of Geophysics Planetary Physics*, *53*, 35–52 (in Chinese).